IEEE Access
Multidisciplinary | Rapid Review | Open Access Journal

Received 13 November 2022, accepted 23 November 2022, date of publication 28 November 2022,
date of current version 7 December 2022.

Digital Object Identifier 10.1109/ACCESS.2022.3225412

RESEARCH ARTICLE

Piston-Seals Friction Modeling Using a Modified Maxwell Slip Formation and Genetic Identification Algorithm

RASHAD MUSTAFA[1], ALI ABDO[2], (Senior Member, IEEE), JAMAL SIAM[3], AND FERIT KÜÇÜKAY[3]

[1]Department of Mechanical and Mechatronics Engineering, Birzeit University, Birzeit 9730000, Palestine
[2]Department of Electrical and Computer Engineering, Birzeit University, Birzeit 9730000, Palestine
[3]Institute of Automotive Engineering, Technical University of Braunschweig, 38106 Braunschweig, Germany

Corresponding author: Rashad Mustafa (rimustafa@birzeit.edu)

This work was supported in part by the Research Committee, Birzeit University.

ABSTRACT Improving spontaneity, shifting control, and efficiency are the main goals of actuators for hydraulic automated transmissions. Friction losses of piston-seals play an essential role in achieving these goals. Therefore, modeling the complex friction behavior of piston seals leads to a better understanding of the determinant factors of energy losses and, consequently, the realization of more efficient transmission actuators. This paper proposes a piston-seal friction model based on the Generalized Maxwell-Slip model. The proposed model introduces an additional hydraulic-pressure dependency that emulates the influence of cylinder-pressure on the displacement variable while accounting for various piston-seal structures. A Genetic Algorithm is also applied to identify and optimize the parameters of the proposed friction model. Simulations with O-Ring, D-Ring, and Bonded Piston seals were developed to show the validity of the proposed model in practical scenarios. The results were also compared with the original Generalized Maxwell Slip friction model to show the superiority of the proposed model in representing the experimental data.

INDEX TERMS Friction modeling, generalized Maxwell model, genetic algorithm optimization, modified generalized Maxwell model, piston seal, proportional-integral observer.

I. INTRODUCTION

Friction is a mechanical, non-linear resistance force that opposes the movement of two bodies moving relative to each other. Friction forces may be desirable in many applications, such as brakes, tires, or clutches. On the other hand, friction has to be minimized as much as possible because it causes wear in mechanical applications and a reduction in efficiency due to the irreversible dissipation of energy. Friction also affects systems where accurate positioning is required and increases the risk of instability. As a result, friction must be reduced or compensated for [1].

For example, automated transmissions are nowadays the most commonly used systems for solving control problems and improving shifting comfort in the vehicle industry. The use of hydraulic actuators in automated transmission systems is a common practice. These actuators include piston seals that exhibit nonlinear friction behavior. Even though friction is essential for the correct operation of various applications that require accurate positioning, it dissipates energy and deteriorates the efficiency of the system. It also plays a determinant role in the structure of pistons-cylinders and seals. Therefore, modeling the frictional behavior of piston seals is a determinant factor for vehicle quality and the development and control of automated transmission.

The following studies showed that friction has many other characteristics, such as adhesion, sliding, nonlinearities, memory, and hysteresis. Richard Stribeck, in 1902, investigated mixed friction, which occurs in the area between adhesion and sliding. This led to the new fundamental Stribeck

The associate editor coordinating the review of this manuscript and approving it for publication was Agustin Leobardo Herrera-May.

curve, which represents the friction force as a function of the sliding speed, [2]. The consequent Dahl model, 1968, was derived from the stress-strain curve characteristics. Dahl discovered that the friction behavior of ball bearings is similar to Coulomb dry friction. He observed that objects return to their original position after small displacements, as in an elastic spring system. In contrast, permanent plastic deformation can occur with large displacements [3]. The following LuGre (Lund and Grenoble University) model, 1995, is based on Dahl's model [4]. LuGre is based on the relative movement between the surfaces. Thus, in contrast to Dahl's model, the LuGre model has a speed-dependent friction function. Furthermore, micro- and viscous friction were considered. However, important effects such as hysteresis were not considered. Leuven model [5], has a more complicated friction model, 2000, which includes non-local memory hysteresis. The model added two state equations to describe the nonlinear aspects of friction and friction forces. The Leuven model was then subjected to further modification [6], to reflect the hysteresis effect with a Maxwell sliding model.

Lately, a new model known as the Generalized Maxwell Slip (GMS) friction model has been introduced, [7]. The core innovation of GMS is that it replaces the Coulomb-slip law with a rate-state law. It includes both velocity and displacement in modeling friction behavior [7]. GMS is now one of the most used models in piston seal design [8], [9], [10]. Therefore, in this study, the GMS model is used as a benchmark for validating the proposed method.

In fact, friction behavior is nonlinear and is influenced by a variety of factors, such as temperature, lubricant, and velocity. Nowadays, the most-known generalized friction model, GMS, is based only on piston displacement and velocity, [7]. Despite the validity of this model in several situations and the use of different identification and optimization methods, it could not exhaustively describe the friction behavior in various piston-seals designs. In addition, one of the main functions of the piston seals is to prevent fluid from flowing out of the cylinder when the piston is moved by the high hydraulic pressure. The increased pressure results in higher adhesion between the piston and the seal. Thus, the friction force between the piston and seal is dependent on the hydraulic pressure of the cylinder.

Despite the advantages of GMS, it was not sufficient to provide a highly precise description of the specific friction behavior of piston-seals. In this work, a Modified Generalized Maxwell Slip (MGMS) friction model is proposed that takes the friction behavior of various piston-seals design into consideration. The MGMS friction model adds a pressure-dependent variable to the original GMS. This action is reflected in the piston-seal structure by adding a spring-damper-mass system with a pressure-dependent spring stiffness. The pressure dependence models the effect of piston displacement obstruction caused by the augmented pressing of the piston against the seal at high pressure.

To this end, GMS had to follow up with the identification and optimization of the piston-seal specific parameters. These steps aim to determine the optimal set of parameters that most closely matches the measured values in order to improve model accuracy. Several methods were used in the identification of GMS parameters. Among these are the friction force prediction models of grey-box and black-box, [11], the robust adaptive observer developed by [12], and the online switching-function presented in [13], which combines a least-square estimator, filtering, and linearization. Numerical optimization techniques used to fit the GMS model parameters for frequencies between 100 and 7000 Hz are discussed in [14]. Several optimization methods were also developed in the mathematics and engineering literature, such as in [15]. These methods were classified as one-dimensional and multi-dimensional, deterministic and stochastic, linear and nonlinear methods [16]. Such as particle swarm optimization [17], and the Genetic Algorithm (GA) as represented in [18] are some of the optimization methods that have been developed. In particle swarm optimization, particles move in a space and each particle searches for the best solution in the search area by changing its velocity. GA is an efficient way to find the global optimum, inspired by natural evolution. Based on numerous literatures, such as [19], GA has been shown to perform better compared to particle swarm optimization by achieving the highest number of best minimum fitness and faster time. The disadvantage of GA is that they are difficult to program and debug, but this can be overcome using GA software toolboxes. Therefore, GA is used to identify and optimize the MGMS parameters (MGMS-GA) in this work.

The objective function of the identification algorithm MGMS-GA is the mean relative error between the experimental data and computed values. The MGMS-GA is implemented using the MatLab Evolutionary Algorithm Toolbox (GEATbx, MatLab), [17], [18]. The proposed model can be integrated into an automated and interactive process to design, evaluate, and select the hydraulic actuator piston-seal with the best type and geometry. In fact, the model can be automated to analyze and determine the effects of friction pressure dependency in different existing and new prototypes of hydraulic-actuator piston-seals during a service period before the seal fails. Thus, the model helps automotive designers and industrial manufacturers interactively model the more precise friction response of their real hydraulic actuators based on experimental measurements.

Furthermore, seal failure is caused by the degradation of material properties and cyclic loading [19]. Therefore, friction is needed to calculate the compressive and contact stresses required in a time-varying reliability model. Furthermore, since the O-ring is replaced on a regular basis, the cyclic loading is no longer important. Therefore, cyclic loading has a relatively small influence compared to compressive and contact stresses [19].

The temperature has a remarkable influence on the sealing performance of rubber O-rings, with temperature changes leading to an increasing damage process [20]. The implemented model focuses only on the pressure effects, which do

reflect the influence of load distribution on the seals and thus the calculation of load cycles.

The paper is organized as follows: Section II introduces an overview of the GMS friction model and the proposed MGMS structure. Section III develops the MGSM with the pressure dependency added to different seal types. Section IV presents the MGSM-GA parameter identification algorithm that accounts for the effect of the seal type. Conclusions are presented in Section V.

II. MODIFICATION OF THE GENERALIZED MAXWELL MODEL

Despite GMS, [7] including the effects of the contact friction forces, it did not take into account the effect of the hydraulic pressure on the piston-seal interface. Obviously, this effect is significant and should be considered in the design of the hydraulic actuators. The hydraulic pressure generates additional lateral forces that change the friction behavior. Clearly, this additional adhesion friction force obstructs the piston displacement in a way that depends on the seal shape and structure, FIGURE 1. For example, the flat D-ring geometry prevents the seal from twisting and rolling and therefore reduces the lateral force compared to the O-Ring seal type, [21]. The MGMS model proposes a new formulation that includes these effects to reduce the modeling errors and enhance the approximation of the measured data.

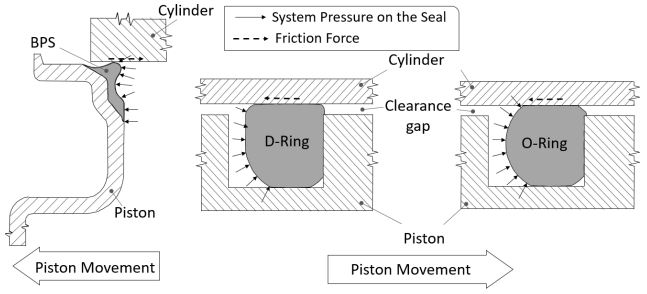

FIGURE 1. System hydraulic pressure exerted on Bonded Piston Seal (BPS), D-Ring, and O-Ring seals.

This section reviews the Generalized Maxwell friction model and the proposed modification that aims to enhance the modeling accuracy in the piston-seal friction formulation.

A. GENERALIZED MAXWELL MODEL

The Generalized Maxwell Friction Model is a variant of the Leuven Model in which the hysteresis term in the Leuven Friction Force Equation is replaced by a superposition of Maxwell Elements. The basic mechanical structure of GMS, FIGURE 2, is a one-dimensional structure with N elastic sliding objects. The objects are placed on rough surfaces with different friction coefficients and are connected to springs with constants k_i. Hereby, each object is characterized by its displacement state-variable ξ_i and subjected to a maximum friction force W_i and an elastic force F_i, FIGURE 3. All objects are simultaneously excited with a displacement z.

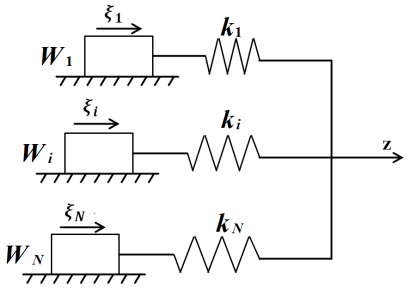

FIGURE 2. Generalized maxwell sliding model for N maxwell elements [7].

The behavior of the Maxwell element i, Figure 2, can be described with Eq. 1 and Eq. 2, [7]:

$$If \ \ |z-\xi_i| < \frac{W_i}{k_i} \ then \begin{cases} F_i = k_i\,(z-\xi_i) \\ \xi_i = const. \end{cases} \tag{1}$$

$$else \begin{cases} F_i = sgn(z-\xi_i)W_i \\ \xi_i = z - sgn(z-\xi_i)\dfrac{W_i}{k_i} \end{cases} \tag{2}$$

with

$$sgn\ (z-\xi_i) = \begin{cases} +1, & z-\xi_i > 0 \\ 0, & z-\xi_i = 0 \\ -1, & z-\xi_i < 0 \end{cases} \tag{3}$$

The two sides of the case statement refer to the behavior during the adhesive phase, *Eq. 1*, and the sliding phase, *Eq. 2*. Small spring forces act on the objects at small displacements z, preventing them from moving, resulting in an adhesion state. If the displacement is increased, the spring forces increase linearly until the first element reaches the friction maximum force W_i. The first element now enters the sliding phase, which means theat ξ_i starts to change and has to be determined. Continuing to increase the displacement action, z, more and more elements will successively move into the sliding phase. As long as only one element has not reached the maximum force W_i, and thus has not yet started to move, the total system of N elements remains in place. When all elements enter the sliding phase, the entire system overcomes the adhesion phase and starts moving.

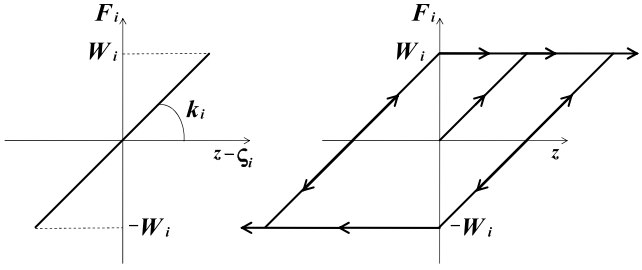

FIGURE 3. Characteristic spring-force *Fi* of a Maxwell element (i) subjected to a displacement stimulus z and maximum friction-force W_i [6].

Thus, using the Maxwell setup in FIGURE 2 and FIGURE 3, the total hysteresis force F_h becomes equal to

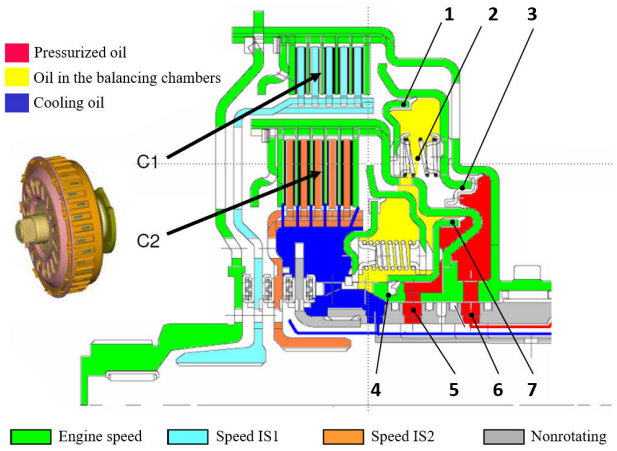

FIGURE 4. Design of the dual-clutch of the 7DCI600 [23].

the sum of all the individual hysteresis forces of all Maxwell elements, [7]:

$$F_h = \sum_{i=1}^{N} F_i \tag{4}$$

B. MEASUREMENT DATA

An Improved Proportional Integral (IPI) observer is used [22] to estimate the friction force acting on the clutch during the shifting process. The observer was tested on experimental data obtained with a GETRAG Dual Clutch Transmission (DCT) in BMW M3 with a petrol engine.

First, the structure of the dual-clutch of the used 7DCI600 DCT is discussed to provide an exact representation of a real example where friction occurs. FIGURE 4 shows the sectional view of the wet double clutch, where the clutch packs C1 and C2 clutches with multi-plate shifting elements, and their connection to the outer disk carrier are shown. The inner disk carriers are each positively connected to the corresponding separate input shafts and therefore rotate at the speeds of IS1 (input shaft 1) or IS2 (input shaft 2). The clutch is supplied with pressure oil via channels 5 and 6. The return springs 2 are located in the oil-filled compensating chambers. The two clutch pistons are sealed with two sealing rings each. In the case of clutch C1, this is done via BPS seals 1 and 3. The same applies to clutch C2 with 4 and 7.

Two external clutch pressure sensors are installed in the mechatronics transmission module, as these are not available in the vehicle CAN BUS. In addition, two signals from the input shaft speed sensor are taken directly from the vehicle CAN BUS.

The experimental data were used to estimate the friction forces of different Freundenberg seals [24] during the shifting process by closing and opening the hydraulic clutch actuator. FIGURES 5 and 6 show the real behavior of the friction forces using an IPI observer for three different piston seal lip designs (D-Ring, O-Ring, and BPS). The measured data are valid for a constant operating temperature. In fact, friction occurs

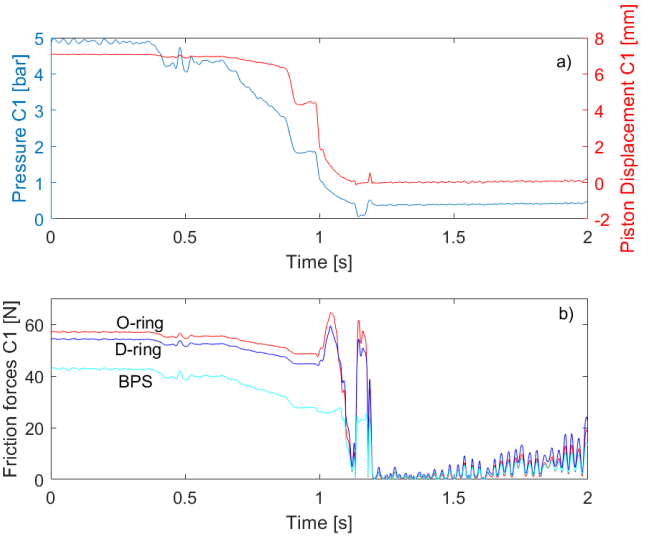

FIGURE 5. Piston displacement with the input pressure of the disengaged clutch and estimated friction forces.

differently for each piston seal type, so each seal structure has different behavior in terms of loss of efficiency, stability, positioning accuracy, and wear.

The main piston dynamic equation of the IPI observer of the dual-clutch index (i) related either to clutch 1 or clutch 2 is updated to include the MGMS friction model as:

$$m_{pi}\ddot{x}_{pi} + k_{pi}x_{pi} = p_{pi}A_{pi} - F_{cf\,1i} + F_{cf\,2i} - F_{Friction(i)} - F_{Ni} - K_{0pi} \tag{5}$$

where $\boldsymbol{m_p}$ is the clutch piston mass, $\boldsymbol{k_p}$ the wire coil return spring stiffness, $\boldsymbol{p_p}$ clutch pressure, and $\boldsymbol{A_p}$ clutch piston area. $\boldsymbol{F_{cf\,1}}$,$\boldsymbol{F_{cf\,2}}$ are centrifugal forces acting on both sides of the piston, which are mainly function from input shaft speeds. The centrifugal forces depend on the design of the dual-clutch, rotational speed, and pressing area. For clutches, the return spring force must be greater than the total centrifugal force acting on the piston. Usually, a hydraulically balanced piston is used to compensate the centrifugal forces in each direction and therefore reduce the required force to return the wire coil spring [25]. $\boldsymbol{K_{0p}}$ is the preload spring force and $\boldsymbol{F_N}$ is the normal clutch force applied to the clutch.

FIGURE 5 (a) and FIGURE 6 (a) show the calculated piston displacement and the applied measured pressure of the clutches to be engaged and disengaged for a reference upshift from first to second gear. A comparison result between the friction forces for the three existing seals is represented in FIGURE 5 (b) FIGURE 6 (b).

The friction forces for different seals and different constant pressures are estimated via the IPI observer and plotted in FIGURE **7**. The figure shows a notable dependence of friction force on the hydraulic pressure of the dual-clutch system.

C. MODIFIED GENERALIZED MAXWELL SLIP MODEL

The idea comes from the need to understand and model the effects of the pressure in the cylinder system, as shown by the

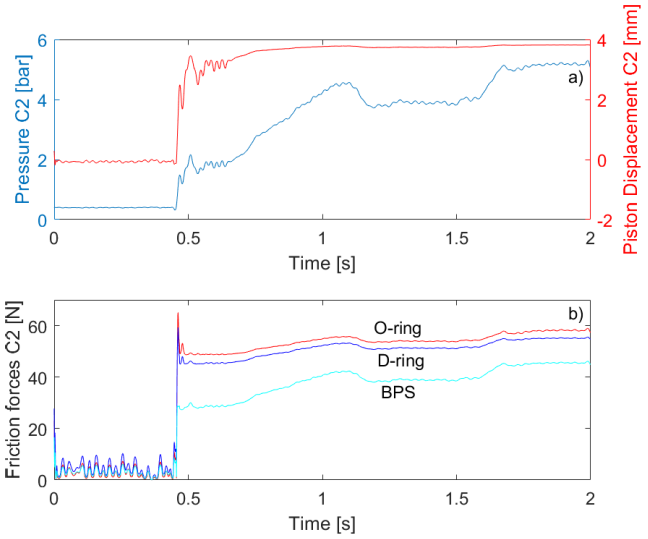

FIGURE 6. Piston displacement with the input pressure of the engaged clutch and estimated friction forces.

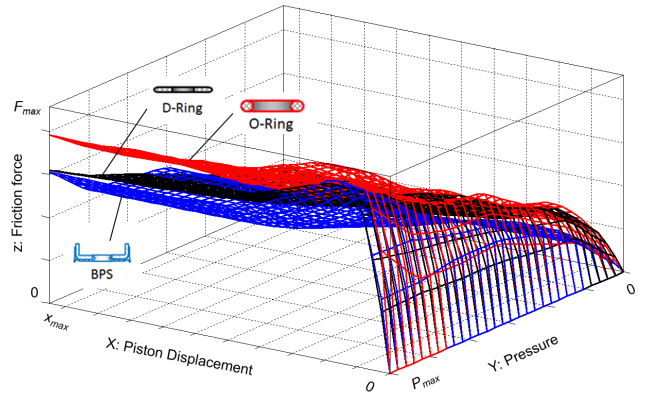

FIGURE 7. Estimated friction force measurements as a function of piston displacement and measured pressure.

measured data, on the performance of the hydraulic actuators and to take into account the different piston-seals structures. In order to include the pressure dependency of friction in the GMS model, some additional parameters such as inertia, damping forces, and speed elements should be considered. The new set of equations should be able to determine the position ξ_i of each moving object as a function of the stimulus z, after the transition from the sticking phase to the sliding phase. Therefore, the Maxwell spring-massless elements are replaced with spring-damper-mass ones, FIGURE 8. The masses of a Maxwell sliding model are measured by their resistance to spring and damping forces. The opposite of mass is massless elements, which have no energy. Moreover, the damping elements are applied to produce a counterbalancing force that reduces the oscillation at each Maxwell element.

To determine the position variable ξ_i in the sliding friction phase, *Eq. 2* must be changed to take into account the spring-damper-mass dynamics. The free-body diagram of the proposed model elements leads to the well-known dynamics

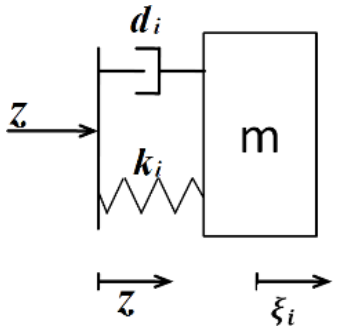

FIGURE 8. Spring-damper-mass system.

characterized by, *Eq.6* and *Eq.7*.

$$\sum F_i = 0 = -m_i\ddot{\xi}_i + k_i\xi_i - k_i z + d_i\dot{\xi}_i - d_i\dot{z} \tag{6}$$

$$\Leftrightarrow \ddot{\xi}_i = \frac{k_i}{m_i}\xi_i + \frac{d_i}{m_i}\dot{\xi}_i - \frac{k_i}{m_i}z - \frac{d_i}{m_i}\dot{z} \tag{7}$$

To adapt the GMS friction principles to the Spring-Damper-Mass (SDM) sliding friction phase *Eq. 2* must be modified as in *Eq. 8* with the $F_{i,STRIBECK}$ given in *Eq. 9*. This formulation allows us to take into account the reduction of the friction force during sliding with increasing displacement.

$$If\ z \geq \frac{W_i}{k_i}\ then\ \begin{cases} F_i = F_{STRIBECK} \\ \xi_i = -\frac{m}{k_i}\ddot{\xi}_i - \frac{d_i}{k_i}\dot{\xi}_i + z + \frac{d_i}{k_i}\dot{z} \end{cases} \tag{8}$$

$$F_{i,STRIBECK} = c\dot{\xi}_i + \left[F_{i,C} + (W_i - F_{i,C})exp\left(-\left(\frac{\dot{\xi}_i}{\dot{\xi}_{iStr}}\right)^{\delta}\right)\right] \times sgn\left(\dot{\xi}_i\right) \tag{9}$$

FIGURE 9 shows that the friction force of a single SDM during adhesion increases linearly according to $F_i = k_i \cdot z$ until the maximum displacement $z_{i,max}$ and thus the maximum force W_i is reached ($t \leq 23ms$). Then, the element starts to slide and therefore, the friction reduces to the Coulomb force $F_{i,C}$ after reaching the Stribeck velocity. It is clear that the Stribeck equation depends on the speed of the mass $\dot{\xi}_i$ and therefore the breakaway force; i.e. the force after which the adhesion is lost, can be represented by the maximum stick phase force W_i.

III. APPLICATION OF MGMS TO PISTON-SEALS

In this section, the work is further developed to model a piston-seal real-friction measurement, considering the effects of hydraulic pressure dependence and seal type.

A. MODELING REAL PISTON-SEAL FRICTION MEASUREMENTS

In this section, the MGMS structure is used to model real piston-seal friction measurements. FIGURE 10(a) shows friction force measurement (IPI observer results) of a D-ring seal at 5-bar with a linear z stimulus to illustrate the modeling procedure without losing generality. This plot shows the initial phase of a linear friction force increase followed by a

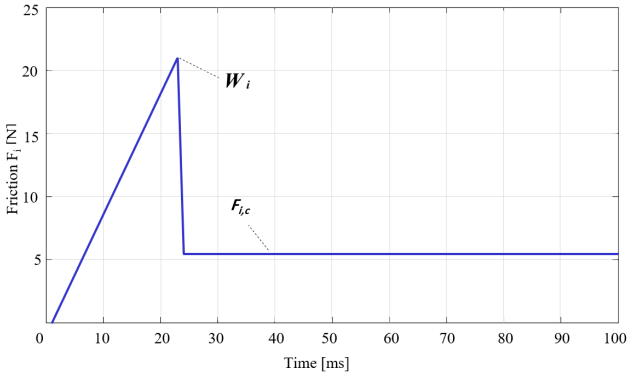

FIGURE 9. Friction force F_i of the spring-damper-mass element at p = 5-bar.

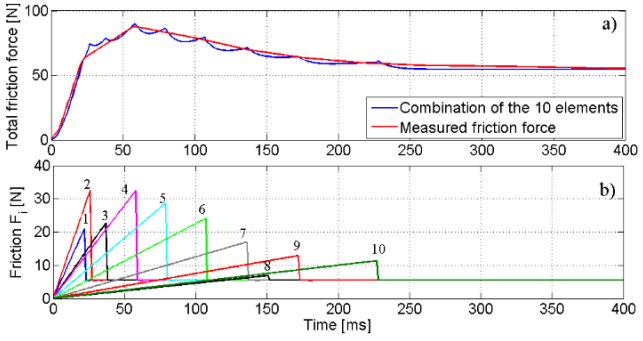

FIGURE 10. (a) Friction force behavior of a D-ring seal at p = 5 bar (b) Characteristics of the friction forces F_i of the ten spring-damper-mass elements used to model the D-ring seal friction force at 5 bar.

second linear friction force increase phase with a different slope. This change indicates an increase in friction force, after reaching the Stribeck velocity, caused by the low influence of the lubricating film in the sliding friction phase. After reaching the maximum value, i.e., the breakpoint, the friction shows a Stribeck-like exponentially decreasing behavior that ends in a constant Coulomb friction value.

A comparison of this behavior with that of a single SMD at the same z-stimulus and pressure value, leads to the belief that a single SMD is inappropriate to model the piston-seal friction forces. As shown in FIGURE 9, in the single SMD characteristic, the Stribeck velocity is reached after a very short time and the exponential decrease of the Stribeck curve to the position of the minimum friction, at Stribeck velocity, occurs instantaneously. Hence, the characteristic of the Stribeck curve can't be observed. Instead, a sharp drop from the limited force $W_i = k_i \cdot z_{i,max} = 21$ N to the Coulomb force $F_{i,C} = 5.46$ N is observed.

Nevertheless, the introduction of additional degrees of freedom using a set of SDM elements to model the measured friction behavior, as in the Maxwell model, could be plausible. The set of required SDM's and relative friction responses should be determined and combined. In FIGURE 10 (a), a system of 10 SDM elements with equal Coulomb friction force and different stick-slip transition points is used to model the measured friction force of the D-ring seal. Hereby, each element has the behavior illustrated in FIGURE 10 (b) and contributes 1/10 of the total Coulomb force. For simulation purposes, the characteristic parameters of *Eq. 8 and Eq. 9* were considered to be:

- Mass of the SDM element $m_{D-RING} = 0.1$ kg
- Damping coefficient of the SDM element $d_{D-RING} = 15$ Ns/m
- Viscous coefficient of friction $c_{D-RING} = 1$ Ns/m
- Stribeck speed $\dot{\xi}_{Str,D-RING} = 0.001$ m/s
- Stribeck exponent Delta $\delta_{D-RING} = 2$

Thus, using the Maxwell setup, the total hysteresis force F_h becomes equal to the sum of all the individual hysteresis-forces (see FIGURE 10 (b)) of all Maxwell elements as in Eq. 4.

B. MODELING THE FRICTION DEPENDENCY ON HYDRAULIC PRESSURE

Up to this point, the actuator-cylinder pressure was assumed to be constant, and the dependence of friction on pressure was ignored. However, the friction forces, FIGURE 7, show that there is a notable dependency of the friction force on hydraulic pressure. The pressure-dependent behavior of the piston-seal friction can be explained mechanically as a preload, which presses the piston more and more strongly against the seal as pressure levels rise (FIGURE 1). Therefore, the friction force increases and augments the obstruction of the piston displacement.

Since the stick-slip transition point and the position and shape of the breakaway force depend on the spring stiffness, the proposed model integrates the effect of pressure (p) in the SDM element k_i as in *Eq. 10* and *Eq. 11*.

$$k_i = k_{i,Ring}\bar{k}_i \tag{10}$$

$$k_{i,Ring} = k_{i,m}p + k_{i,b} \tag{11}$$

Here the variable $k_{i,Ring}$, is a pressure-dependent line, $k_{i,m}$, and $k_{i,b}$ denote the line parameters and are identical for all elements i of a defined sealing type. The factor $\bar{k}_i$ characterizes the stiffness factor of a specific SDM element.

Moreover, the Coulomb friction force, $F_{Ci,Ring}$, of each SDM element i, is considered to be pressure-dependent as in Eq. 13. Accordingly, the point of transition, of each SDM friction force, to the Coulomb level depends also on pressure.

$$F_{Ci,Ring} = (F_{Ci,m}p + F_{Ci,b})/i \tag{12}$$

where $F_{Ci,m}$ and $F_{Ci,b}$ represent the Coulomb forces pressure dependency parameters, these parameters are assumed to be identical for all the SDM elements of a defined seal type.

C. SEAL-TYPE FRICTION MODEL IDENTIFICATION

In the previous subsection, the variables $k_{i,Ring}$, $F_{Ci,Ring}$ were assumed to be seal-type specific. i.e., the characterization of the pressure effect on the friction forces was assumed to be based on the type of the piston-seal. Therefore, identification and optimization methods must be used to determine the parameters of *Eq. 10 - Eq. 12* that best achieve the

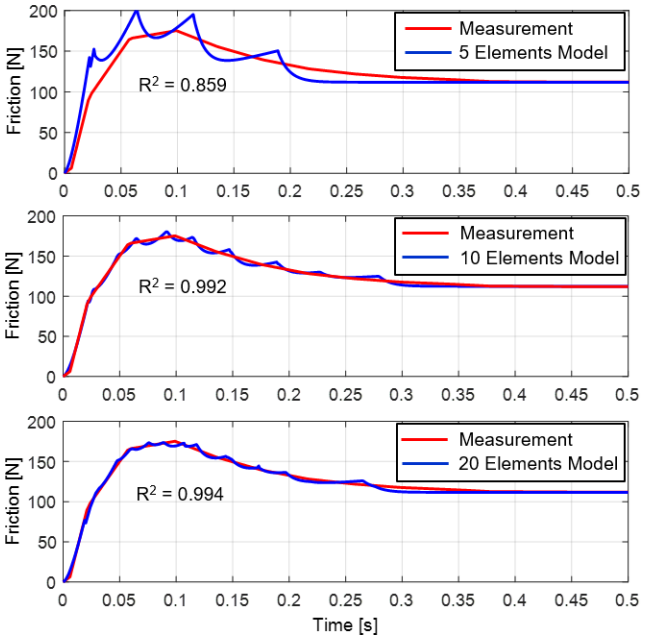

FIGURE 11. Effect of the number of SDM elements, n, on the modeling accuracy of the friction-force measurements of a Bonded Piston Seal (BPS), for n = 5, 10, and 20 at p = 25bar.

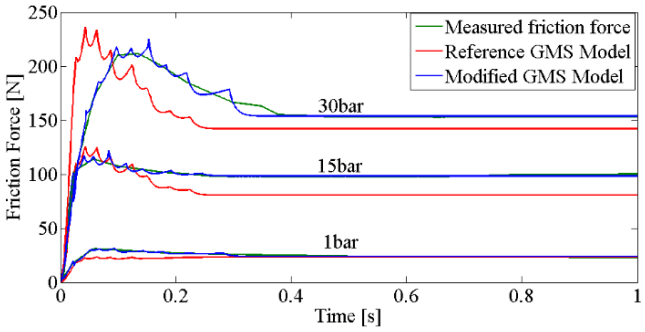

FIGURE 12. Friction behavior of the BPS for various pressures with 10 structure elements for the modified and reference model.

friction behavior defined by each seal type measurement, FIGURE 5. In this study, a Genetic Algorithm based on the fitness function defined in [26] and [27], and the GEATbx (Genetic Evolutionary Algorithm Toolbox) were used to identify the model parameters. The fitness function considers, as an objective function, the mean relative error between the experimental measurements and simulation values. The pressure-dependent parameters were assumed to be equal for all the SDM elements of a defined seal type.

Obviously, the number of SDM elements, n, affects the modeling accuracy and the number of parameters to be identified, N_{ident}, which is given by $N_{ident} = 2n+4$. For example, the total number of identification parameters for 10 SDM elements is 24, i.e. 10 characteristic SDM stiffness parameters, $\bar{k}_i$, 10 maximum spring travels $z_{i,max}$ that define the maximum force $W_{i,max} = \bar{k}_i z_{i,max}$ and stick-slip transition point, and the pressure-dependency parameters $F_{C,b}$, $F_{C,m}$, $k_{i,m}$, and $k_{i,b}$. The simulation plots, FIGURE 11, show the effect of the

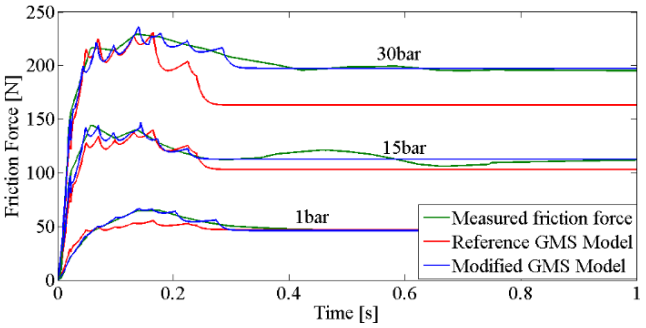

FIGURE 13. Friction behavior of the O-Ring various pressures with 10 structure elements for the modified and reference model.

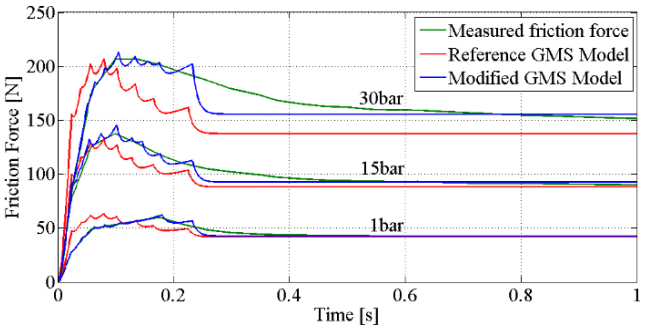

FIGURE 14. Friction behavior of the D-Ring various pressures with 10 structure elements for the modified and reference model.

number of SDM elements on the modeling accuracy of a Bonded Piston seal (BPS) for *n = 5, 10, and 20,* respectively. These plots show that the modeling accuracy increases with, *n*. On the other hand, the use of the high value of, *n*, is not advisable since it increases the N_{ident} and computation cost. FIGURE 11 also show that the measurement data of the BPS is modeled with very good accuracy using *n = 10*. In fact, higher values of, *n*, lead to small accuracy improvements.

In each case, the value of R^2 is calculated for the fitting. The number of Maxwell elements depends on the type of application and the time scale of the system in which the seals are applied. In this paper, the seals are applied in an automated vehicle transmission where shift comfort and spontaneity are important. With a number of 10 Maxwell elements, very good accuracy can be obtained ($R^2 > 0.99$).

IV. COMPARISON WITH GMS

FIGURES 12, 13, and 14 show the friction behavior for different pressures and different types of seals. With the help of the MGMS, it is possible to adjust the friction process during the maximum effective friction forces and thus during the breakaway phase with only 10 elements. Furthermore, the relative error between the experimental data and the calculated values should be minimal from the beginning to the end of the transient phase (t < 0.2 s) and the same during the steady state (t > 0.5 s). Thus, the increasing behavior of the friction force at the beginning of the adhesion phase was satisfied by summing the effects of the individual hysteresis forces of the 10 Maxwell elements as in *Eq. 1* and *4*. Moreover,

increasing the Maxwell elements can enhance the model's accuracy.

In addition, the modified friction model can deal with all seal shapes, such as those presented in FIGURE 1, in which the friction behavior under the effects of pressure is not the same. Here, the most influential behaviors to be considered in hydraulic cylinders are seal stretching, squeezing, and rolling. The fluctuations of the sealing O-Ring in FIGURE 13 during the sliding phase, which can be observed due to the rolling movements, cannot be measured since the force sensor measures the Coulomb force during the sliding phase. Increasing the hydraulic pressure leads to a higher adhesion between the piston and the seal and thus a higher friction force. The flat D-ring geometry, for example, prevents the seal from twisting and rolling and therefore reduces the frictional forces compared to O-ring seals.

As shown in the figures, the results of the proposed method (MGMS) are very close to the measurement data. On the other hand, the standard GMS model cannot give good results with increasing pressure.

V. CONCLUSION

This paper reviewed the most commonly used friction models in the literature. A modified friction model with additional pressure dependence based on the GMS is also presented. The friction model parameters involved in each seal lip design were determined using the GA identification technique. The friction behavior for each seal slip design was compared with the measurement data for different seal lip designs and shows that the novel model can predict all friction properties for all seal types. Moreover, this study concludes that a very good approximation of real friction processes is possible even with a small number of Maxwell elements. Finally, the modified friction model can describe friction dynamic characteristics with high nonlinearity and many parameters depending on the used seal types and therefore can be used in many design and control purposes in many industrial applications, such as automated transmissions.

In order to improve the implemented model, the temperature stress will be considered in the follow-up work by performing different temperature tests.

REFERENCES

[1] K. Åström and C. C. de Wit, "Revisiting the LuGre model—Stick slip motion and rate dependence," *IEEE Control Syst. Mag.*, vol. 28, no. 6, pp. 101–114, Dec. 2008.

[2] V. Popov, *Contact Mechanics and Friction: Physical Principles and Applications*. Berlin, Germany: Springer-Verlag, 2010.

[3] H. Olsson, K. J. Åström, C. C. de Wit, M. Gäfvert, and P. Lischinsky, "Friction models and friction compensation," *Eur. J. Control*, vol. 4, no. 3, pp. 176–195, Jan. 1998.

[4] C. C. de Wit, H. Olsson, K. J. Astrom, and P. Lischinsky, "A new model for control of systems with friction," *IEEE Trans. Autom. Control*, vol. 40, no. 3, pp. 419–425, Mar. 1995.

[5] J. Swevers, F. Al-Bender, C. G. Ganseman, and T. Projogo, "An integrated friction model structure with improved presliding behavior for accurate friction compensation," *IEEE Trans. Autom. Control*, vol. 45, no. 4, pp. 675–686, Apr. 2000.

[6] V. Lampaert, J. Swevers, and F. Al-Bender, "Modification of the Leuven integrated friction model structure," *IEEE Trans. Autom. Control*, vol. 47, no. 4, pp. 683–687, Apr. 2002.

[7] F. Al-Bender, V. Lampaert, and J. Swevers, "The generalized Maxwell-slip model: A novel model for friction simulation and compensation," *IEEE Trans. Autom. Control*, vol. 50, no. 11, pp. 1883–1887, Nov. 2005.

[8] Y. F. Liu, J. Li, Z. M. Zhang, X. H. Hu, and W. J. Zhang, "Experimental comparison of five friction models on the same test-bed of the micro stick-slip motion system," *Mech. Sci.*, vol. 6, no. 1, pp. 15–28, Mar. 2015.

[9] F. Soleymani, S. M. Rezaei, S. Sharifi, and M. Zareinejad, "Position control of a servo-pneumatic actuator using generalized Maxwell-slip friction model," in *Proc. 4th Int. Conf. Robot. Mechatronics (ICROM)*, Tehran, Oct. 2016, pp. 246–251.

[10] L. Pálfi, T. Goda, K. Váradi, and E. Garbayo, "FE prediction of hysteretic component of rubber friction," *Adv. Tribol.*, vol. 2012, Mar. 2012, Art. no. 807493.

[11] K. Worden, C. X. Wong, U. Parlitz, A. Hornstein, D. Engster, T. Tjahjowidodo, F. Al-Bender, D. D. Rizos, and S. D. Fassois, "Identification of pre-sliding and sliding friction dynamics: Grey box and black-box models," *Mech. Syst. Signal Process.*, vol. 21, no. 1, pp. 514–534, Jan. 2007.

[12] S. Grami and P. Bigras, "Identification of the GMS friction model based on a robust adaptive observer," *Int. J. Model., Identificat. Control*, vol. 5, no. 4, p. 297, 2008.

[13] Y. Gharbia and S. Grami, "Identification of GMS friction model using a new switching function: Experimental investigation," *Int. J. Model., Identificat. Control*, vol. 27, no. 1, p. 31, 2017.

[14] R. Esmaeeli and S. Farhad, "Parameters estimation of generalized Maxwell model for SBR and carbon-filled SBR using a direct-frequency DMA measurement system," *Mech. Mater.*, vol. 146, Jul. 2020, Art. no. 103369.

[15] G. Fontecha Dulcey, X. Fischer, P. Joyot, and G. Fadel, "Support for decision making in design of composite laminated structures. Part 2: Reduced parametric model-based optimization," *Appl. Composite Mater.*, vol. 26, no. 2, pp. 663–681, Apr. 2019.

[16] T. Terlaky, M. F. Anjos, and S. Ahmed, *Advances and Trends in Optimization With Engineering Applications* (MOS-SIAM Series on Optimization), vol. 24. Philadelphia, PA, USA: SIAM, 2017.

[17] J. Kennedy and R. Eberhart, "Particle swarm optimization," in *Proc. IEEE ICNN*, vol. 4, Nov./Dec. 1995, pp. 1942–1948.

[18] J. Nowaková and M. Pokorný, "System identification using genetic algorithms," in *Proc. Int. Conf. Parallel Problem Solving Nature*, vol. 5, 2014, pp. 413–418.

[19] S. P. Lim and H. Haron, "Performance comparison of genetic algorithm, differential evolution and particle swarm optimization towards benchmark functions," in *Proc. IEEE Conf. Open Syst. (ICOS)*, Dec. 2013, pp. 41–46.

[20] A. Chipperfield, P. Fleming, and H. Pohlheim, "Genetic algorithm toolbox: For use with MATLAB; user's guide (version 1.2)," Dept. Autom. Control Syst. Eng., Univ. Sheffield, Sheffield, U.K., Tech. Rep., 1994.

[21] P. Hartmut, *Evolutionary Algorithms—Methods, Operators, Practical Examples*. Berlin, Germany: Springer-Verlag, 1999.

[22] B. Liao, B. Sun, M. Yan, Y. Ren, W. Zhang, and K. Zhou, "Time-variant reliability analysis for rubber O-ring seal considering both material degradation and random load," *Materials*, vol. 10, no. 10, p. 1211, Oct. 2017.

[23] B. Sun, M. Yan, Q. Feng, Y. Li, Y. Ren, K. Zhou, and W. Zhang, "Gamma degradation process and accelerated model combined reliability analysis method for rubber O-rings," *IEEE Access*, vol. 6, pp. 10581–10590, 2018.

[24] R. Flitney, *Seals and Sealing Handbook*, 6th ed. Amsterdam, The Netherlands: Elsevier, 2014.

[25] R. Mustafa and F. Küçükay, "Model-based estimation of unknown contact forces acting on a piston in dual clutch transmission," in *Proc. SAE World Congr. Exhib.*, vols. 2012–0110, 2012.

[26] S. Rinderknecht, "Getrag powershift 7DCI600—DCT for high efficiency and dynamics in inline powertrains," in *Proc. CTI Symp. Innov. Automot. Transmisisons*, Berlin, 2007.

[27] J. Trabert and J. Kohn, "Sealing of transmission pistons with PTFE for increased gear shift comfort," *ATZ Worldwide eMagazine*, vol. 113, no. 3, pp. 36–39, Mar. 2011.

[28] R. Mustafa, T. Kassel, G. Alvermann, and F. Küçükay, "Nonlinear modelling and unknown input estimation of an electro-hydraulic system for a dual clutch transmission," in *Proc. ASME Int. Mech. Eng. Congr. Expo.*, Vancouver, BC, Canada, Jan. 2010, pp. 361–370.

[29] D. Goldberg and K. Sastry, *Genetic Algorithms*. New York, NY, USA: Springer, 2007.

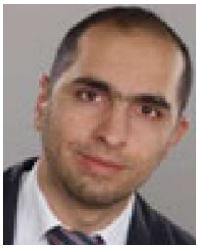

RASHAD MUSTAFA received the B.Sc. degree in mechanical engineering from Mutah University, Jordan, in 2005, the M.Sc. degree in mechatronics from the University of Duisburg–Essen, Germany, in 2007, and the Ph.D. degree in automotive engineering from the Technical University of Braunschweig, Germany, in cooperation with Volkswagen AG, in 2014. He worked in the system engineering hybrid module development at Schaeffler AG, Germany, from 2014 to 2018. He has been working as an Assistant Professor at Birzeit University, since 2018.

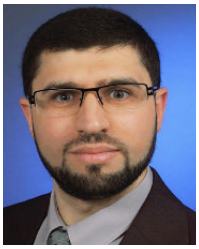

ALI ABDO (Senior Member, IEEE) received the B.Sc. degree in electronic engineering from Al-Quds University, Palestine, in 2005, the M.Sc. degree in power and automation from the University of Duisburg–Essen, Germany, in 2008, and the Ph.D. degree in electrical engineering from the Institute for Automatic Control and Complex Systems (AKS), University of Duisburg–Essen, in 2013. He is currently an Associate Professor at Birzeit University, Palestine. His research interests include model-based fault diagnosis, fault detection in lateral vehicle dynamics, fault detection in switched systems, power systems, and system identification. He is also a member of the Institute of Electrical Engineers of Japan (IEEJ). He got many awards and scholarships throughout his study.

JAMAL SIAM received the second degree in electronics and computer engineering from the Bari University of Study, Italy, in 1991, and the Ph.D. degree in biomedical engineering from the University of Tel Aviv, Israel, in 2015. He worked as a System Engineer, until 1994. Since 1994, he has been a Lecturer with the Department of Electrical and Computer Engineering, Birzeit University, Palestine, where he is currently an Associate Professor. His research interests include filter design, signal and systems, control systems, and biomedical engineering.

FERIT KÜÇÜKAY received the Ph.D. degree in mechanical engineering from the Department of Mechanical Engineering, Technical University of Munich. After that, he worked with BMW at 'Chassis Pre Development' and 'Power Train Development,' from 1985 to 1997. He is currently a Managing Director with the Institute of Automotive Engineering, Technical University of Braunschweig, Germany. His research interests include vehicle dynamics, chassis engineering, powertrain, driver assistance systems, and objectification of subjective driver-, driving environs-, and driven vehicle- parameters, as well as representative requirements based on customers' use.